0026-895X/08/7405-1203–1214$20.00
MOLECULAR PHARMACOLOGY
Copyright © 2008 The American Society for Pharmacology and Experimental Therapeutics
Mol Pharmacol 74:1203–1214, 2008

Vol. 74, No. 5
47837/3394712
Printed in U.S.A.

1-[6-[[(17β)-3-Methoxyestra-1,3,5(10)-trien-17-yl]amino]hexyl]-1*H*-pyrrole-2,5-dione (U73122) Selectively Inhibits Kir3 and BK Channels in a Phospholipase C-Independent Fashion

Angelika Klose, Tobias Huth, and Christian Alzheimer

Department of Physiology, University of Kiel, 24098 Kiel, Germany

Received April 9, 2008; accepted August 4, 2008

ABSTRACT

1-[6-[[(17β)-3-Methoxyestra-1,3,5(10)-trien-17-yl]amino]hexyl]-1*H*-pyrrole-2,5-dione (U73122) is widely used to inhibit phospholipase C (PLC)-mediated signaling, but we and others have also reported a PLC-independent block of Kir3 channels in native cells. To elaborate on this major side effect, we examined the action of U73122 and 1-[6-[[(17β)-3-methoxyestra-1,3,5(10)-trien-17-yl]amino]hexyl]-2,5-pyrollidinedione (U73343), a structurally related but not PLC-inhibiting analog, on Kir1.1, Kir2.1, or Kir3.1/3.2 channels expressed in HEK293 cells. Both compounds (10 μM) displayed an unusual degree of selectivity for Kir3, superior even to that of tertiapin, which discriminates between Kir3 and Kir2 but also inhibits Kir1.1. Recordings from mutant Kir2 and Kir3 channels showed that U73122 is unlikely to block Kir3 by interfering with binding of phosphatidylinositol 4,5-bisphosphate, and U73122 did not seem to act like a pore blocker. U73122 and U73343 also unexpectedly suppressed Ca^{2+}-activated K^+ channels of the large-conductance type (MaxiK, BK) in a PLC-independent fashion. In single-channel recordings, both compounds significantly decreased open probability of BK channels and slowed their ultrafast gating ("flickering") at very depolarized potentials. Alignment of the amino acid sequences of Kir3 and BK channels suggested that the highly selective effect of U73122/U73343 is mediated by a homologous domain within the long C-terminal ends. In fact, mutations in the C-terminal region of Kir2 and Kir3 channels significantly altered their sensitivity to the two compounds. Our data strongly caution against the use of U73122 when exploring signaling pathways involving Kir3 and BK channels. However, the apparent binding of U73122/U73343 to a common structural motif might be exploited to develop drugs selectively targeting Kir3 and BK channels.

Phospholipase C (PLC) regulates phosphatidylinositol 4,5-bisphosphate (PIP_2) levels in the plasma membrane and generates the second messengers inositol 1,4,5-trisphosphate (IP_3) and diacylglycerol. The PLC inhibitor U73122 is widely used to explore the various facets of PIP_2-associated signaling, including Ca^{2+} release from IP_3-sensitive calcium stores, diacylglycerol-mediated activation of protein kinase C, and PIP_2-dependent regulation of ion channel activity. However, the selectivity of U73122 has been disputed (Vickers, 1993; Jin et al., 1994; Mogami et al., 1997; Horowitz et al., 2005). In the ion channel field, a particular concern is that U73122 seems to exert a direct inhibition of Kir3 (G protein-coupled inwardly rectifying potassium channel) channels that is not associated with its action on PLC (Cho et al., 2001; Lei et al., 2001; Meyer et al., 2001; Filippov et al., 2004; Sickmann et al., 2008). In a previous study in cardiac cells, Cho et al. (2001) proposed that U73122 blocks Kir3 channels by interfering with their PIP_2 binding site. Here, we used a heterologous expression system in combination with whole-cell and single-channel recordings to elaborate on the reported effect of U73122 on Kir3 channels and to elucidate the putative site of drug action at the channel molecule. We also screened for other ion channels that might possibly be affected by U73122 in a similar PLC-independent fashion. Whereas the compound proved highly selective even within the Kir channel family, we made the surprising and novel observation that the compound is also a direct blocker of large-conductance Ca^{2+}-activated K^+ (BK, MaxiK, Slo1) channels.

This work was supported by the University of Kiel.
A.K. and T.H. contributed equally to this work.
Article, publication date, and citation information can be found at http://molpharm.aspetjournals.org.
doi:10.1124/mol.108.047837.

Materials and Methods

Cell Culture and Transfection. HEK293 cells were maintained at 37°C in 5% CO_2 in Dulbecco's modified Eagle's medium (Invitro-

ABBREVIATIONS: PLC, phospholipase C; PIP_2, phosphatidylinositol 4,5-bisphosphate; IP_3, inositol 1,4,5-trisphosphate; U73122, 1-[6-[[(17β)-3-methoxyestra-1,3,5(10)-trien-17-yl]amino]hexyl]-1*H*-pyrrole-2,5-dione; U73343, 1-[6-[[(17β)-3-methoxyestra-1,3,5(10)-trien-17-yl]amino]hexyl]-2,5-pyrollidinedione; HEK, human embryonic kidney; PCR, polymerase chain reaction; DMSO, dimethyl sulfoxide; *m*-3M3FBS, 2,4,6-trimethyl-*N*-[3-(trifluoromethyl)phenyl]benzenesulfonamide; BK channel, large conductance Ca^{2+}-activated K^+ channel; V_h, holding potential; I-V, current-voltage; NP_o, mean open probability; TEA, tetraethylammonium; NEM, *N*-ethylmaleimide; GEPD, generalized epilepsy and paroxysmal dyskinesia.

gen, Carlsbad, CA) and supplemented with 10% fetal bovine serum (Biochrom, Berlin, Germany) and 1% penicillin/streptomycin solution (Biochrom). For stable ROMK (Kir1.1) cell lines, media were supplemented with hygromycin B (0.05 mg/ml) and Zeocin (0.1 mg/ml), and stable BK$\alpha+\beta$1 cell lines media were supplemented with G418 (Geneticin; 0.5 mg/ml; all antibiotics from Invitrogen). For transient transfection, cells were plated in 3.5-cm dishes (Falcon; BD Biosciences Discovery Labware, Bedford, MA) and the next day transfected with Superfect (QIAGEN, Hilden, Germany) or Nanofectin (PAA, Pasching, Austria) with 0.5 to 1 μg of cDNA of each construct and with 0.5 μg of c-enhanced green fluorescent protein (Clontech, Mountain View, CA) according to the manufacturer's protocol. Recordings were carried out 2 to 3 days after transfection.

Molecular Biology. Kir1.1 in pcDNA5/pFRT-lacZneo stable transfected in HEK293 cells was kindly provided by K. Steinmeyer (Sanofi-Aventis, Frankfurt, Germany). Kir2.1, bicistronic Kir3.1/3.2, and 5-HT_{1A}-receptor in pcDNA3 were kindly provided by A. Karschin (Institute of Physiology, University of Würzburg, Germany). BK$\alpha+\beta$1 in pcDNA3 stable transfected in HEK293 cells and BKα (hSLO1-GFP) were gifts from A. Schromm (Research Center, Borstel, Germany). IK1 in pcDNA3 was a gift from S. Werner (Institute of Cell Biology, ETH Zurich, Switzerland). KCNQ1/E1 and KCNQ2/3 in pFrog were kindly provided by M. Schwake (Department of Biochemistry, University of Kiel, Germany). Alignment for protein sequence comparison was performed with the use of MATCH-BOX (Depiereux et al., 1997).

Point mutations were created using the site-directed mutagenesis kit QuikChange II XL (Stratagene, La Jolla, CA). Deletion constructs ($BK_{1\text{-}I322}$, $BK_{1\text{-}L360}$, $BK_{1\text{–}435A}$, $BK_{1\text{-}E576}$, and $Kir3.1_{1\text{-}G431}$) were created via PCR. The resulting PCR products were subcloned into pENTR-D-TOPO and then pcDNA DEST47 (both Invitrogen). Kir3.1/3.2-Kir2.1 chimeras ($Kir3.1/3.2_{Kir2.1\text{-}PIP}$, Kir3.1/3.2-Kir2.1, Kir2.1-Kir3.1/3.2) were created using a two-step fusion PCR technique (LongRange PCR Kit; QIAGEN). The resulting PCR products were subcloned into pENTR-D-TOPO and then pcDNA DEST47. All mutations were confirmed by sequencing (Eurofins MWG Operon, Ebersberg, Germany). To obtain $Kir3.1_{Kir2.1\text{-}PIP}$ chimeras, the PIP_2 domain of Kir2.1(K207–L245) was transferred into Kir3.1(G207–L246) and Kir3.2(G216–L255). Primer sequences are given in Table 1.

Reagents and Solutions. U73122 and U73343 were purchased from BIOMOL Research Laboratories (Hamburg, Germany) or from Sigma (Deisenhofen, Germany). Both compounds were divided into aliquots using chloroform and dried under a nitrogen atmosphere at 50°C in a shaker. Lyophilized aliquots were stored at −20°C until use. On the day of use, pellets were dissolved in DMSO at a concentration of 10 mM under vigorous vortexing at 35°C. Aqueous solutions were freshly prepared from DMSO solutions and used within 30 min. *m*-3M3FBS was purchased from Sigma. Stock solution (50 mM) was prepared in DMSO. In all experiments, maximum final DMSO concentration was ≤0.1%. Control experiments with 0.1% DMSO alone in the different recording configurations (whole cell, $n = 9$; single channel, $n = 7$) excluded nonspecific drug effects mediated by the solvent (data not shown). Compositions of bath and pipette solutions are given in Table 2. All ingredients were bought from Sigma.

Electrophysiology. Transfected HEK293 cells were identified under an inverted fluorescence microscope (Zeiss, Jena, Germany). Whole-cell current signals were recorded in voltage-clamp mode at room temperature (21–22°C). Recordings were sampled at 20 kHz and filtered at 5 kHz using an Axopatch 200B amplifier in conjunction with a Digidata 1322A interface and pClamp9.2 software (all from Molecular Devices/MDS Analytical Technologies, Sunnyvale, CA). Patch pipettes were made from borosilicate glass (Harvard Apparatus, Edenbridge, UK) using a DMZ-Universal Puller (Zeitz, Munich, Germany) and had a resistance of 3 to 5 MΩ when filled with pipette solution. Access resistance in the whole-cell configuration was 5 to 12 MΩ before series resistance compensation (75 to 80%). Cell capacitance was approximately 10 to 20 pF. Recordings typically started 5 min after obtaining whole-cell access. Drugs were applied by means of a rapid, gravity-driven Y-tube system. Single-channel recordings were performed in the inside-out configuration. Pipettes were coated internally with Sigmacote (Sigma, Deisenhofen, Germany) and dried at 55°C for 24 h as described previously (Huth et al., 2008). Pipette resistance was typically 10 to 20 MΩ when filled with pipette solution. Recordings were sampled at 100 kHz and filtered at 10 kHz. Single-channel data were analyzed (level and jump detection, open probability histograms, dwell time histograms)

TABLE 1
Primer sequences

$Kir3.1_{Kir2.1\text{-}PIP}$	
Forward 1	CACCatgtctgcactccgaagg
Reverse 1	ccacatcaagcaagttttccgtccctcatggaaat
Forward 2	ggggagtacatccccttggaccaacttgaactggat
Reverse 2	ctatgtgaagcggtcagagttcatttttc
$Kir3.2_{Kir2.1\text{-}PIP}$	
Forward 1	CACCatggccaagctgacagaa
Reverse 1	ccacatcaagcagagtttcccatcccgcatggagat
Forward 2	ggggagtacatcc-ccttgaaccagacggatatcaac
Reverse 2	ctaaactttggattcattctcc
$Kir3.1_{C179_V179}$Kir2.1	
Forward 1	CACCatgtctgcactccgaagg
Reverse 1	cttcgccatcttcgccatgacgcagccgatgaggaaagcgtc
Forward 2	gacgctttcctcatcggctgcgtcatggcgaagatggcgaag
Reverse 2	ctatatctccgattctcgccttaaagg
$Kir3.2_{C188_V179}$Kir2.1	
Forward 1	CACCatggccaagctgacagaatcc
Reverse 1	cttcgccatcttcgccatgacgcatcccaccatgaatgcatt
Forward 2	aatgcattcatggtgggatgcgtcatggcgaagatggcgaag
Reverse 2	ctatatctccgattctcgccttaaagg
$Kir2.1_{Y326_F328}$Kir3.1	
Forward 1	CACCatgggcagtgtgagaaccaac
Reverse 1	ttctaaagaaattacagggaagtagcggtgaccccagagaat
Forward 2	attctctggggtcaccgctacttccctgtaatttctttagaa
Reverse 2	ctatgtgaagcggtcagagttcatttttct
$Kir2.1_{Y326_T337}$Kir3.2	
Forward 1	CACCatgggcagtgtgagaaccaac
Reverse 1	ctccagggtcaggacaggtgtgtagcggtgaccccagagaat
Forward 2	attctctggggtcaccgctacacacctgtcctgaccctggag
Reverse 2	ctaaactttggattcattctccaggtttgc

using standard functions of pClamp 9.2 software. Statistical analyses were performed with the use of one-way analysis of variance followed by a post hoc Tukey's test or paired t test, as appropriate. Data are expressed as mean ± S.E.M., with significance set at $p < 0.05$. Curves were fitted using Origin Pro7G software (OriginLab Corp., Northampton, MA) or pClamp 9.2.

Results

Inhibition of Kir3.1/3.2 Channels by U73122. Previous studies (from our laboratory and others) in native cardiac and neuronal cells pointed to a suppression of Kir3 channels by U73122 that was apparently not related to inhibition of PLC (see Introduction). To further investigate this puzzling effect of U73122 in a defined expression system, we performed whole-cell recordings from HEK293 cells that transiently expressed Kir3.1/3.2 channels and 5-HT_{1A} receptor. Serotonin is known to activate Kir3 channels in a fast, membrane-delimited fashion by G protein $\beta\gamma$ dimers released from (or spatially rearranged in) 5-HT_{1A} receptor-bound $G_{i/o}$ heterotrimers (Sodickson and Bean, 1998). When applied at a holding potential (V_h) of −70 mV, serotonin (20 μM) produced a fast inward current that partially desensitized (Fig. 1A), as reported previously (Sickmann and Alzheimer, 2002, 2003). Determination of the current-voltage (I-V) relationship by means of a voltage ramp protocol revealed the characteristic inward rectification of Kir3 (Fig. 1B). When added to the serotonin-containing superfusion medium, a near-saturating concentration of U73122 (10 μM, Fig. 1E) suppressed the K^+ current. Neither tertiapin (30 nM), a highly potent and selective blocker of Kir3 (Jin and Lu, 1998), nor Ba^{2+} (200 μM and 2 mM), which is fairly selective for inward rectifier K^+ currents at the low concentration, produced further inhibition of the current, indicating an already complete block by U73122 alone (Fig. 1, A and D). To demonstrate that this effect occurred in a PLC-independent fashion, we repeated the above experiment using U73343 (10 μM), a structurally related analog that does not affect PLC (Fig. 6B). As for U73122, inhibition by U73343 of the K^+ current was virtually complete, because again, additional Ba^{2+} did not further diminish the current (Fig. 1, B and D). We then determined dose-response relationships for Kir3 current inhibition by U71322 and U73343, using guanosine 5′-*O*-(3-thio)triphosphate-filled cells to prevent current desensitization (Sickmann et al., 2008). Kir3 channels were activated maximally with serotonin, before the compounds were applied at increasing concentrations (0.1–30 μM) in a stepwise fashion (Fig. 1C). Intermediate drug-washout was not possible, because both compounds produced largely irreversible effects. In a separate experiment, no appreciable recovery was observed within 30 min of drug washout ($n = 3$ for each compound; data not shown). Dose-response curves were fitted to a standard logistic equation, yielding IC_{50} values of 0.54 ± 0.04 μM ($n = 7$) and 0.55 ± 0.02 μM ($n = 7$) for U73122 and U73343, respectively (Fig. 1E).

To explore the blocking effect of the two compounds at the single-channel level, we performed single-channel recordings in the inside-out configuration, with serotonin (20 μM) and GTP (0.3 mM) present in pipette solution and bath (intracellular) solution, respectively. Under these conditions, the mean open probability of the Kir3.1/3.2 channels in the patch (NP_o) was 0.22 ± 0.04 ($n = 20$). When the intracellular side of the patch was exposed to U73122 (10 μM) or U73343 (10 μM), Kir3 channel activity was strongly suppressed and the NP_o values declined to 0.05 ± 0.01 ($n = 13$, $p < 0.01$) and 0.04 ± 0.01 ($n = 7$, $p < 0.001$), respectively (Fig. 2, A and B). By contrast, the current amplitude of single-channel openings, which averaged 2.55 pA at −70 mV, was not affected by the compounds. Dwell-time histograms revealed two open and four closed time constants (Fig. 2, C and D). Application of U73343 reduced the shorter open dwell time from 0.14 to 0.04 ms, whereas the longer was only slightly reduced (1.33 to 1.10 ms). All four closed time constants present under control conditions (0.03, 0.24, 2.4, and 30.9 ms) were increased by U73343, with a bias toward the longer ones (0.07, 0.5, 7.8, and 104.0 ms).

We next examined whether other members of the Kir family would be also subjected to PLC-independent suppression by U73122 and U73343. However, in contrast to their potent blocking action on Kir3 channels, the compounds did not affect K^+ currents generated by HEK293 cells expressing

TABLE 2
Composition of bath and pipette solutions for different recording conditions
pH was adjusted to 7.4 (bath) and 7.2 (pipette).

	Kir1wc	Kir2wc	Kir3wc	BKwc1	BKwc2	BKsc	Kir3sc
				mM			
External solutions							
KCl	120	120	120	5		5	120
NaCl	5	5	5	140		140	5
$CaCl_2$	2	2	2	1.6		1	2
$MgCl_2$	2	2	2	2		3	2
HEPES	5	5	5	5		5	5
Glucose	10	10	10	5		5	10
Mannitol	50	50	50				50
Internal solutions							
KCl	120			117	140	140	
Potassium gluconate		135	135				135
NaCl	15	4	2	10	15	15	2
$CaCl_2$				4.3	0.3	0.3	
$MgCl_2$	4	3	3	5	1	1	3
HEPES	5	5	5	10	5	5	5
EGTA		5	5	5			5
NaGTP		0.3	0.3				0.3
Na_2ATP	4	2	2	2			2

wc, whole-cell; sc, single channel.

either Kir1.1 (ROMK; data not shown) or Kir2.1 (IRK) channels (Fig. 3C). The strikingly different effect on the closely related Kir2.1 and Kir.3.1/3.2 channels might possibly point to an interaction of the compounds with the PIP_2 binding site, as originally proposed by Cho et al. (2001). Whereas PIP_2 is tightly bound to Kir2.1 channels, giving rise to a constitutive inward rectifier K^+ current, the normally weak interaction between PIP_2 and Kir3 requires stabilization by G protein $\beta\gamma$ subunit for channel opening. We thus examined the effects of U73122 and U73343 on genetically modified Kir2.1 and Kir3.1/3.2 channels that displayed inverse PIP_2 affinities. It has been reported previously that an isoleucine-to-leucine mutation at position 232 of Kir3.2 affords the channel higher PIP_2 affinity (Zhou et al., 2001; Du et al., 2004), whereas a leucine-to-isoleucine mutation at position 222 of Kir2.1 loosens the normally tight PIP_2 binding to the channel (Zhang et al., 1999; Du et al., 2004). In addition, we used a chimera of Kir3.1/3.2 and Kir.2.1 in which a 40-amino acid sequence involved in PIP_2 binding was interchanged (Zhang et al., 1999). To demonstrate the functionality of the mutation, we compared the effect of the PLC activator *m*-3M3FBS (50 μM) on K^+ currents generated by $Kir2.1_{wt}$ and $Kir2.1_{L222I}$. Whereas the activator did not affect wild-type channels ($n = 6$), it inhibited mutant channels by 46.5 ± 5.2% ($n = 6$, $p < 0.02$; Fig. 3, A and B inset). By contrast, U73122 ($n = 5$) and U73343 ($n = 4$) remained as ineffective on $Kir2.1_{L222I}$ as they had been on $Kir2.1_{wt}$ (U73122, $n = 7$; U73343, $n = 14$; Fig. 3, C and D). Vice versa, U73122 and U73343 produced identical suppression of K^+ currents generated by wild-type and mutant Kir3.2 channels independent of whether the latter carried the I232L mutation or whether they were chimeric constructs (Fig. 4, A and B). As expected from the enhanced PIP_2 binding to chimeric channels, constitutive channel activity before drug application was already increased, thereby reducing the apparent amplitude of the serotonin response (Fig. 4A). These data suggest that U73122 and U73343 are unlikely to affect channel gating through an interaction with the PIP_2 binding site.

Inhibition of BK Channels by U73122 and U73343. In addition to suppressing Kir3 channels, both compounds turned out to be inhibitors of large-conductance Ca^{2+}-activated K^+ (BK, MaxiK) currents, which were recorded from HEK293 cells transfected with BK α-subunit alone or, in some initial experiments, together with β1-subunit. Because

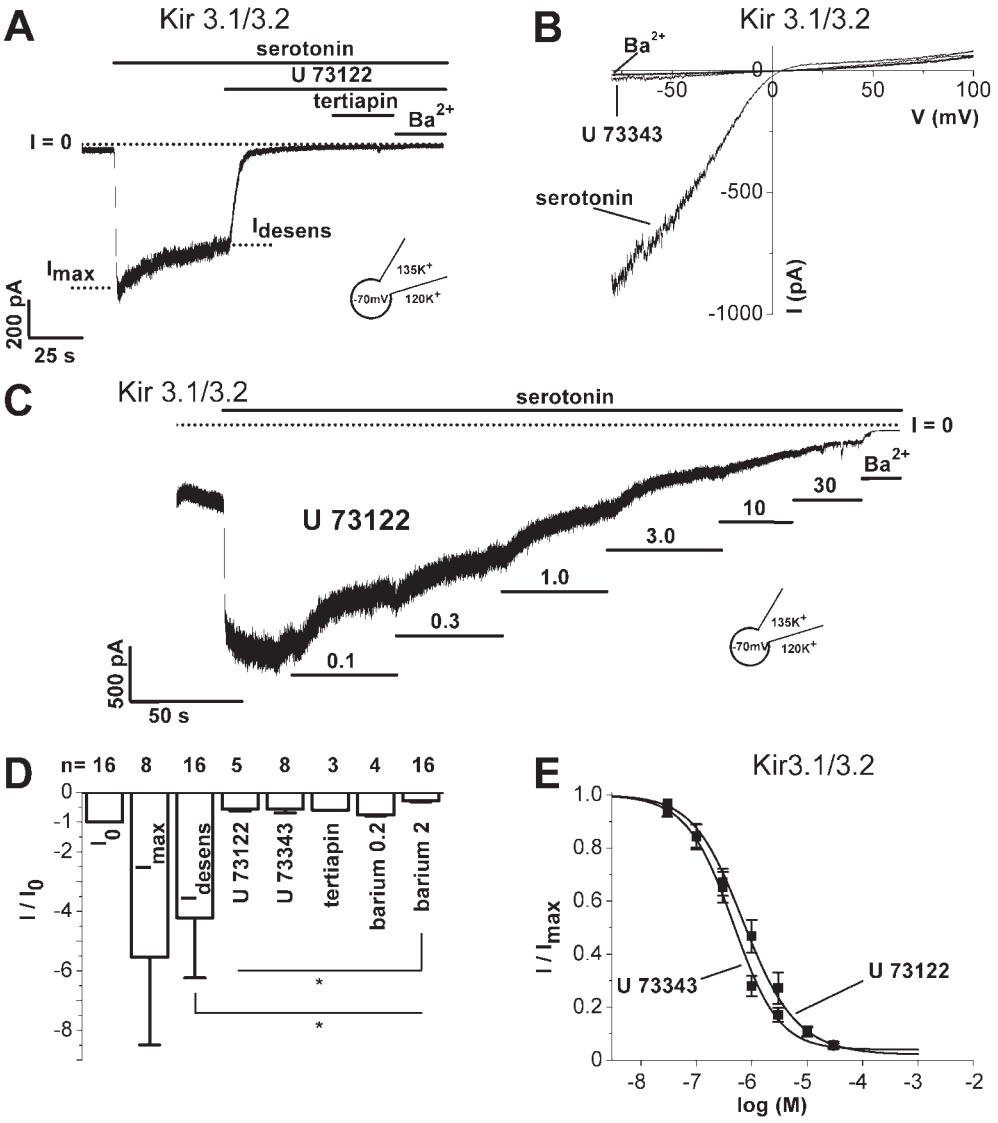

Fig. 1. Inhibition by U73122 and its non PLC-inhibiting analog, U73343 of K^+ currents generated by Kir3.1/3.2 heteromultimeric channels transiently expressed in HEK293 cells. A, K^+ currents were evoked by bath application of serotonin (20 μM) acting on coexpressed $5\text{-}HT_{1A}$ receptors. Dashed lines indicate maximum current (I_{max}) and partially desensitized current (I_{desens}). Application of U73122 (10 μM) completely abrogated serotonin-induced K^+ current as indicated by the lacking effect of potent Kir3 channel blockers tertiapin (30 nM) and Ba^{2+} (200 μM). Inset depicts schematic drawing of whole-cell configuration indicating V_h and K^+ gradient. B, voltage ramps revealed characteristic inward rectifying I-V relationship of Kir3 current, which was fully blocked by U73343 (10 μM). C, incremental suppression of Kir3 currents in guanosine 5′-*O*-(3-thio)-triphosphate-treated cells by stepwise increases in U73122/U73343 concentration. Note reduction of noise as channel activity is progressively suppressed. D, histogram summarizes experiments exemplified in A showing significant reduction of normalized amplitudes of Kir3 currents by U73122 and U73343. Additional current suppression by 2 mM Ba^{2+}, but not 0.2 mM Ba^{2+}, probably reflects unspecific ion channel block at higher concentration. Number (n) of experiments is given above each column. Inhibition by each blocker was tested for significance with respect to I_{desens} and effect of 2 mM Ba^{2+}. E, using a logistic equation, dose-response curves for U73122 and U73343 were determined from experiments such as exemplified in C. Relative inhibition of serotonin-evoked Kir3 current amplitude was plotted as a function of drug concentration. Hill coefficient was 0.8 and 1.1 for block by U73122 and U73343, respectively. $* p < 0.05$

the absence or presence of the auxiliary subunit did not affect the drug response, data from both groups were lumped together. U73122 (10 μM) and U73343 (10 μM) inhibited BK currents with a time course similar to that of Kir3 suppression (Fig. 5, A and B), and the remaining BK current was suppressed by TEA (10 mM). Time constants for BK current suppression by U73122 and U73343 were 2.8 $\pm$ 0.4 s (n = 5) and 4.2 $\pm$ 0.9 s (n = 4). For comparison, the corresponding time constants for Kir3 current suppression were 4.1 $\pm$ 0.5 s (n = 7) and 3.7 $\pm$ 0.5 s (n = 7), respectively. To determine the effective dose range, we superfused HEK293 cells with increasing concentrations of U73122 or U73343 in a stepwise fashion (0.3–10 μM). Dose-response relationships were constructed by plotting relative BK current amplitude as a function of drug concentration, yielding IC_{50} values of 2.3 μM for U73122 and 19.3 μM for U73343 (Fig. 5C).

Current responses to voltage ramps from −100 to +100 mV were used to determine the I-V relationship of BK current. Figure 5D depicts I-V curves obtained in the absence and presence of U73122 (10 μM) and TEA (10 mM). Because BK currents might partially decline during prolonged depolarization, we also used depolarizing voltage steps in lieu of

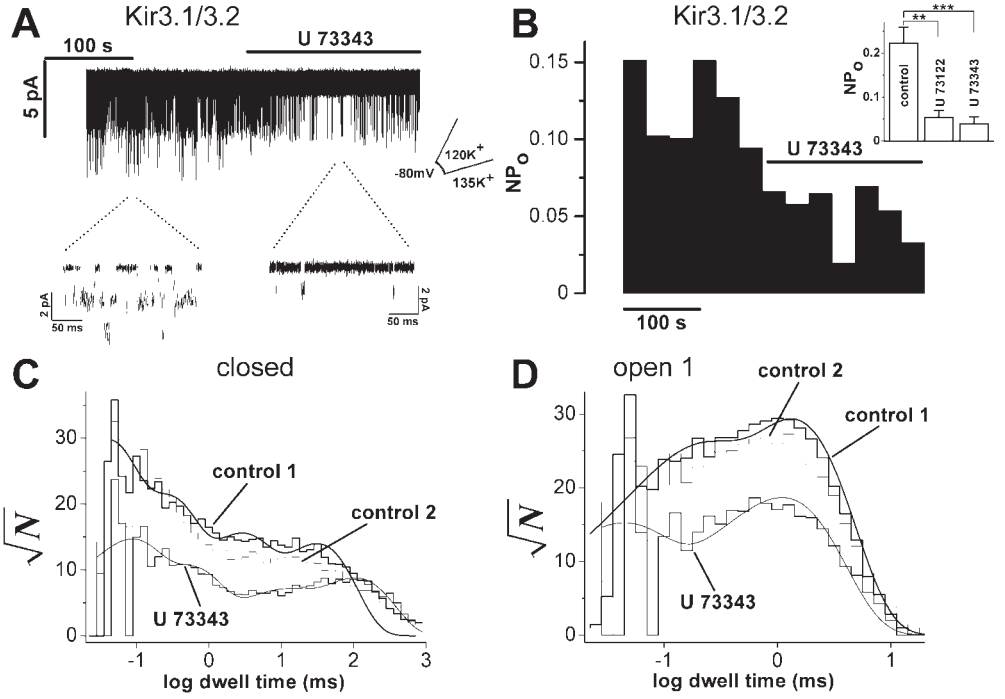

Fig. 2. In inside-out patches, U73122/U73343 decreased open probability of serotonin-activated Kir3.1/3.2 channels. A, single-channel activity before and during application of U73343 (10 μM) is shown at low temporal (continuous recording) and high temporal resolution (insets below). B, histogram shows decrease in open probability of all active channels in the patch (NP_o) during application of U73343 (data from A). Inset summarizes significant reduction of open probability by U73122 (n = 13) and U73343 (n = 7) in all patches examined. C and D, open and closed dwell-time histograms were fitted best using two and four dwell-time constants, respectively. Control 1 and control 2 refer to two subsequent control recording periods, each lasting 150 s, to demonstrate stable recording conditions before drug application. ** p < 0.01, *** p < 0.001

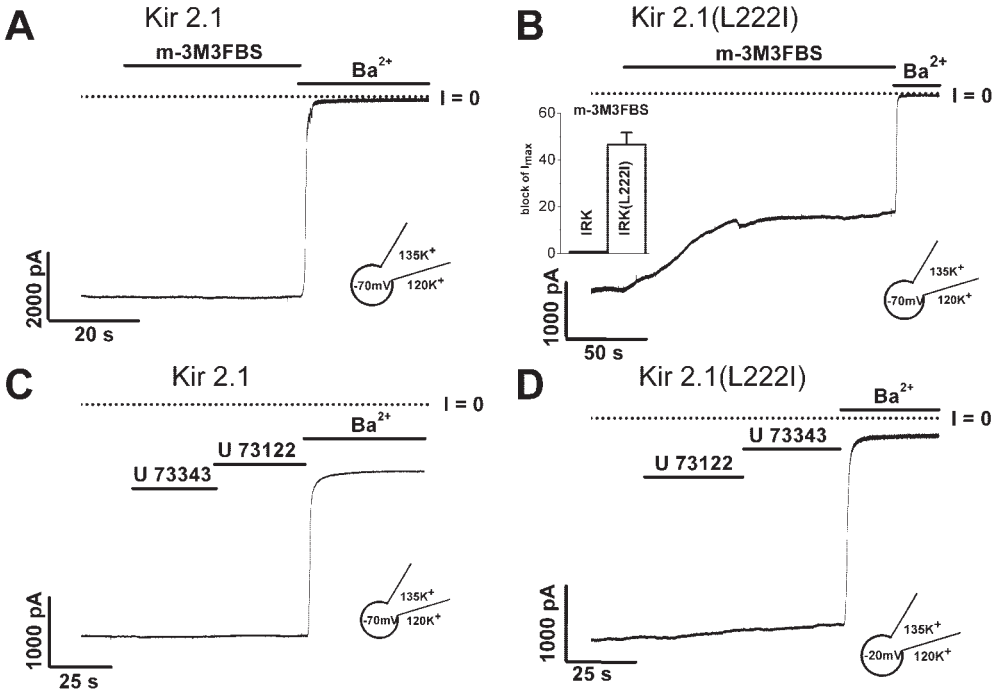

Fig. 3. Mutation decreasing their PIP_2 affinity did not render Kir2.1 channels sensitive to U73122/U73343. A, lacking effect of PLC activator m-3M3FBS (50 μM) on K^+ current generated by wild-type Kir2.1. B, in HEK293 cells expressing $Kir2.1_{L222I}$ mutant channels, m-3M3FBS was capable of reducing K^+ current as a result of reduced PIP_2 affinity, demonstrating functionality of mutation. Inset summarizes data from all experiments (n = 6). C and D, representative recordings showing that wild-type and mutant Kir2.1 channels were both insensitive to U73122 and U73343.

ramps, which allowed us to detect peak BK current amplitudes (Fig. 5E). We then calculated BK conductance with the use of equation $G = I/(V - E_{rev})$, where I is the peak amplitude (I_{max}) of BK current at command potential V and E_{rev} is the equilibrium potential for K^+ under our experimental conditions (−84 mV). U73122 reduced maximum BK conductance from 101.7 ± 15.1 nS ($n = 9$) to 61.6 ± 11.3 nS ($n = 9$, $p = 0.0025$). The relative decrease is illustrated in Fig. 5F, where G_{max} of control was set to 1.0. The data points were fitted by a standard sigmoidal (Boltzmann) relation of the form $G/G_{max} = 1/[1 + \exp((V_{mid} - V)/k)]$, where V_{mid} is the midpoint of the activation curve and k is a slope factor. It is noteworthy that U73122 also produced a significant leftward shift of V_{mid} from 22.8 ± 6.5 to 6.0 ± 5.9 mV ($n = 9, p < 0.05$). This shift of current activation in the hyperpolarizing direction became immediately apparent, when we replotted the activation curves after matching them with respect to peak conductance (Fig. 5F, inset).

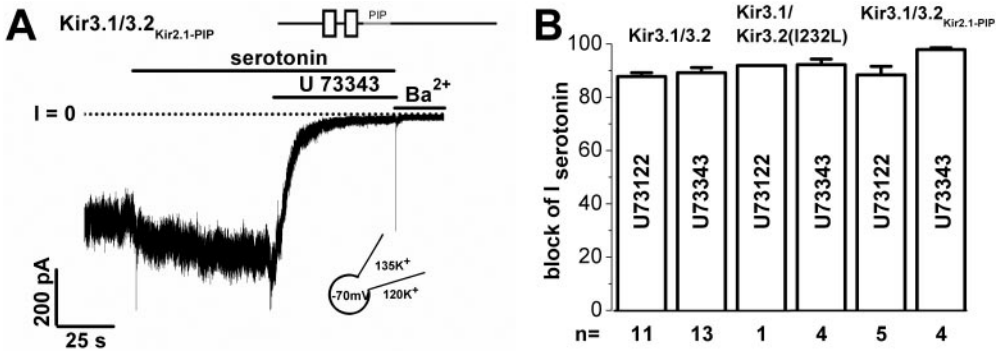

Fig. 4. Mutations increasing PIP_2 affinity of Kir3.1/3.2 channels did not alter inhibition by U73122/U73343. A, K^+ current generated by Kir3 chimeras whose low-affinity PIP_2 binding domain was replaced with high-affinity domain of Kir2.1 was fully blocked by U73343 (10 μM). B, histogram summarizing percentage inhibition of K^+ currents shows equal potency of U73122 and U73343 in wild-type, chimeric, and Kir3.1/3.2$_{I232L}$ mutant channels.

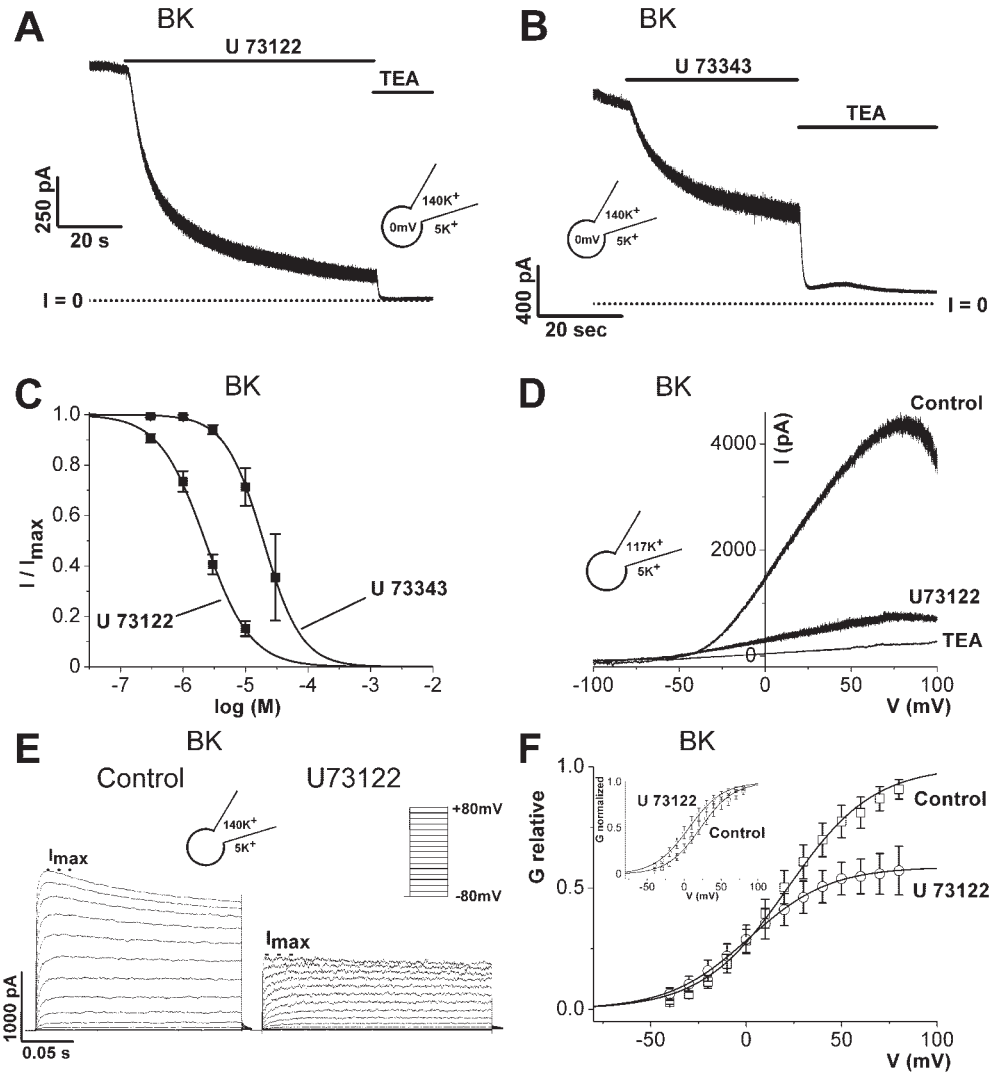

Fig. 5. U73122 and U73343 inhibited BK (MaxiK) channels in HEK293 cells. A and B, application of U73122 (10 μM, A) or U73343 (10 μM, B) inhibited BK current. Insets depict recording conditions. BK current was completely suppressed by TEA (10 mM). C, dose-response relationships for inhibition of BK current by U73122 and U73343. Data points represent mean ± S.E.M. of at least $n = 6$ independent measurements. Curve fitting was performed using a standard logistic equation. Hill coefficient was 1.1 and 1.4 for block by U73122 and U73343, respectively. D, I-V relationships of BK currents under control conditions, in the presence of U73122 and during TEA. E, reduction by U73122 of BK currents evoked by voltage steps to various test potentials (inset). F, activation curves of BK currents before and during U73122 ($n = 9$). To demonstrate the leftward shift of current activation by U73122, curves were replotted after matching their relative G_{max} (inset).

Viewed from a structural standpoint, U73122 is an *N*-substituted maleimide that differs from U73343 in only one double bond that renders the former chemically reactive and, like *N*-ethylmaleimide (NEM), might cause alkylation of cysteine residues (Fig. 6B). By contrast, U73343 is the non-reactive succinimide analog. It is noteworthy that many side effects of U73122 have been attributed to alkylation of various proteins. Because U73122 was found to exert stronger inhibition of BK currents compared with U73343 (see above), we wondered whether part of the block might result from alkylation of cysteine residues. We therefore compared the inhibitory effect of U73122 with that of NEM, which contains the same reactive group. When applied at 100 μM, at which it has been shown before to modify KCNQ2/3 current (Horowitz et al., 2005), NEM failed to influence BK current ($n = 3$, Fig. 6A). Thus, chemical modification of the channel protein is probably not responsible for the stronger blocking effect of U73122 compared with that of U73343. On a cautionary note, however, a comparison between the effects of U73122 and NEM could be compromised by the fact that the structure of U73122 might target its alkylating group more efficiently to a specific cysteine in the channel molecule than NEM alone would be capable of.

It has been proposed that, under certain conditions, U73122 might cause a weak *activation* of PLC (Horowitz et al., 2005). Although we were not aware of any study reporting a PIP_2 dependence of BK gating, we wanted to rule out the possibility that the higher efficacy of U73122 to inhibit BK channels, compared with U73343, is attributable to a gradual depletion of PIP_2. We therefore employed the PLC activator *m*-3M3FBS (50 μM), which completely abrogated K^+ currents generated by Kir3.1/3.2 channels ($n = 5$, Fig. 6C). By contrast, we failed to observe any discernible effect of the PLC-activator on BK current ($n = 7$, Fig. 6D).

To gain further insight into the mechanism of block, we recorded single BK channels in the inside-out configuration. The I-V relationship of BK channels displayed saturation at approximately +50 mV and a negative slope with further depolarization (Fig. 7, A and C), consistent with the behavior of the BK current on the whole-cell level (Fig. 5D). The gradual decline of BK channel current with strong depolarization away from E_{rev}, which apparently uncouples the measured current amplitude from driving force, has been reported before (Schroeder and Hansen, 2007). Seen from a mechanistic perspective, this phenomenon has been attributed to very fast gating ("flickering") of the selectivity filter, which is believed to become unstable as it (and/or the adjacent cavity) is depleted of potassium ions (Schroeder and Hansen, 2007). U73343 (10 μM) and, more so, U73122 (10 μM)—consistent with its higher efficacy at the whole-cell level—had two distinct effects on BK channel gating. First, both compounds produced a significant reduction in NP_o at all voltages tested (Fig. 7, B and D). Dwell time analysis of channel gating at +20 mV showed that U73122 prolonged closed times and reduced open times (Fig. 7, E and F; open dwell times: control, 0.12, 1.40, and 7.83 ms; U73122, 0.05, 0.24, and 0.96 ms; closed dwell times: control, 0.04, 0.40, and 3.55 ms; U73122, 0.07, 1.33, and 8.92 ms). Second, the apparent decrease of the I-V relationship at potentials positive to +50 mV was partially (U73343) or fully (U73122) reversed (Fig. 7, B and C). A comparison of the current traces recorded at +80 mV in the absence and presence of U73122 illustrates its striking effect on channel gating (Fig. 7, A and B). Under control conditions, the channel seemed to gate in a very fast ("flickering") mode (see above) that gave rise to pronounced noise at the open level. U73122 substantially slowed gating, thereby preventing channel "flickering" so that individual gating events could be fully resolved. As a consequence, single-channel currents seemed much higher in amplitude (Fig. 7B), and the I-V relationship became linear in this voltage range as predicted by the increase in driving force (Fig. 7C). It is noteworthy that spontaneous switches to slow gating occurred only very infrequently during control recording ep-

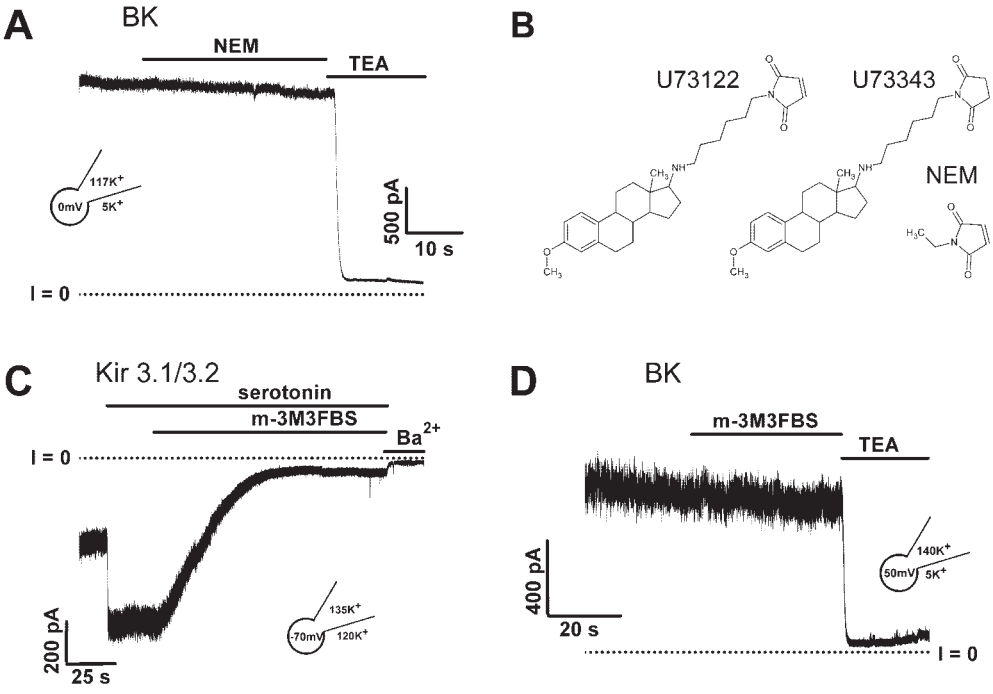

Fig. 6. Inhibition of BK current by U73122 was not associated with alkylation of cysteine residues or PLC activation. A and B, BK current was not affected by NEM (100 μM), which is endowed with same reactive group as U73122, whereas U73343 is rendered inactive by the lack of one double bond (B). C and D, the PLC inhibitor *m*-3M3FBS (50 μM) reliably decreased Kir3 current (C) but failed to affect BK current (D).

ochs. It therefore seems likely that U73122 and U73343 stabilized the slow gating mode.

Structural Elements Involved in Drug Action. With respect to other K^+ channel families, the compounds did not affect K^+ currents produced by Ca^{2+}-activated K^+ channels of intermediate conductance (IK1; data not shown). In addition, U73343 had no effect on K^+ currents generated by KNCQ1/E1 or KCNQ2/3 channels (data not shown). Although it did not considerably inhibit these currents either, U73122 displayed minor and ambiguous side effects in some cells (data not shown), consistent with previously published findings (Horowitz et al., 2005). Finally, a previous study reported that U73122 had no appreciable effect on transient outward and delayed rectifier K^+ currents (Cho et al., 2001). The most parsimonious explanation for the high selectivity of U73122/U73343 for Kir3 and BK channels, which belong to different ion channel families (inward rectifier K^+ channels versus Ca^{2+}- and voltage-activated K^+ channels), would be that these two particular channels share a homologous site of drug action. To determine whether Kir3 and BK channels display sequence homologies within one or more of these regions, we aligned their amino acid sequences and compared them with those of Kir1 and Kir2 channels, which are not sensitive to U73122 (Fig. 8A). As indicated by the stretches of amino acids marked in blue and red, Kir3 and BK channels did indeed show several sequence similarities within their long C terminus. We then mapped these apparent homologies onto schematic drawings of the secondary structure of BK and Kir3 channels. As indicated by the circles in like colors, sequence similarities were found between the regulator of conductance for K^+ (RCK)1 domain of BK channels and a PIP_2- and Na^+-binding domain of Kir3 channels, and between the region linking RCK1 and RCK2 domains of BK channels and a G$\beta\gamma$-binding motif of Kir3 channels (Fig. 8B). To test the hypothesis that U73122 binds to one of this regions to inhibit BK channel activity, we examined several channel constructs that were truncated at different positions along the C terminus as indicated by the green bars in Fig. 8B. These experiments were based on a now controversial study by Piskorowski and Aldrich (2002), who reported nearly unaltered electrophysiological properties of BK channel constructs in which the entire cytoplasmic C terminus was deleted. In our hands, none of the constructs yielded functional BK channels, although each BK construct had the ER export sequence (Kwon and Guggino, 2004) attached to the truncated C terminus to enhance surface expression. Our data agree well with those from a report by Schmalhofer et al. (2005), who also failed to detect channel activity in truncated $BK_{1–323}$, $BK_{1–343}$, $BK_{1–441}$, and $BK_{1–651}$ constructs.

In view of the lacking functionality of the BK constructs,

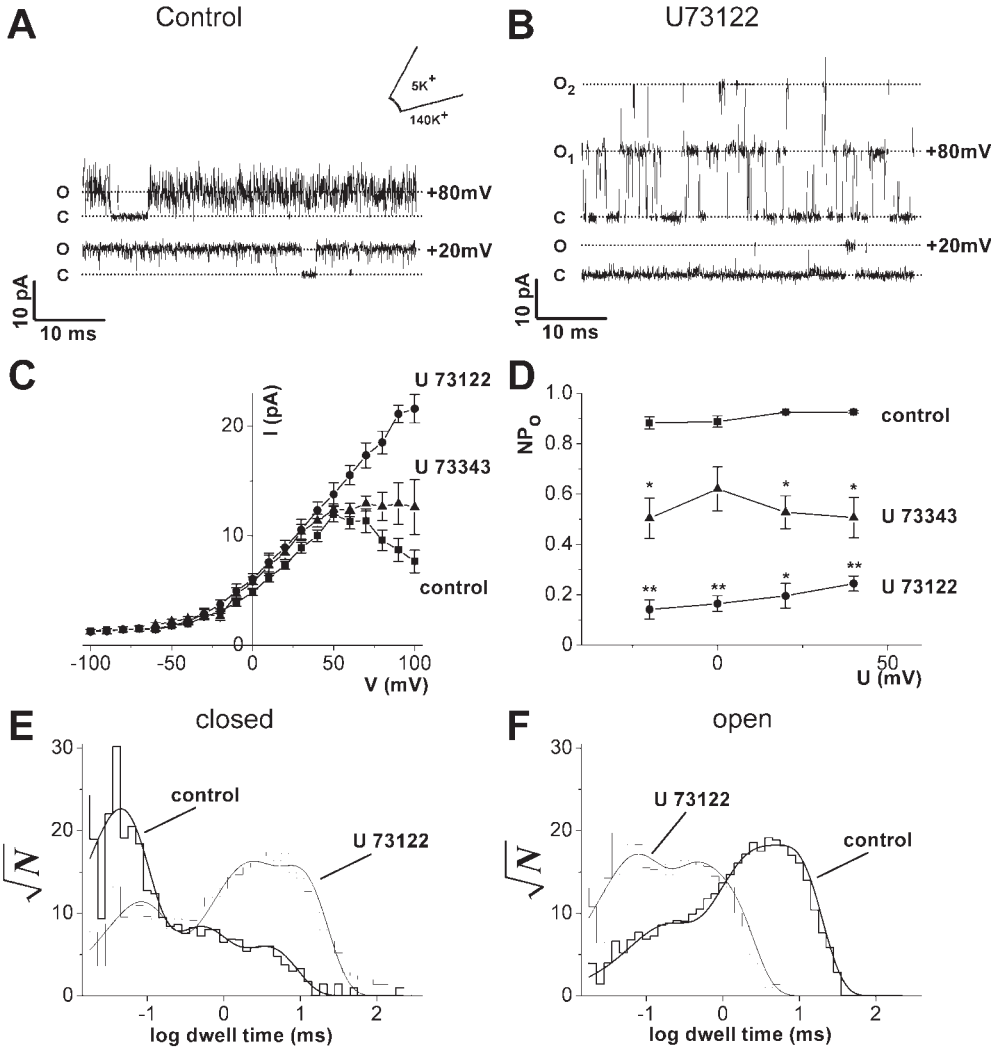

Fig. 7. Dual effect of U73122/U73343 on single BK channels. A, single-channel activity at two V_h (+20 and +80 mV) under control conditions. B, U73122 (10 μM) strongly reduced open probability at +20 mV and caused transition from very fast gating ("flickering") to slower gating mode at +80 mV. C, single-channel I-V relationships. Note that apparently negative slope of control I-V curve (n = 14) positive to +50 mV was partially and fully reversed by U73343 (10 μM, n = 10) and U73122 (10 μM, n = 7), respectively. D, decrease of NP_o by U73122 and U73343. Each data point represents mean ± S.E.M. of at least three independent measurements. E and F, closed and open dwell-time histograms were best fitted using three dwell time constants. $* p < 0.05$, $** p < 0.01$

we designed several mutant Kir3/Kir2 channels to identify the structural elements involved in the action of U73122/U73343 (Fig. 9A), based on the above alignment and published data (Huang et al., 1995; Slesinger et al., 1995). Truncation of the C terminus of Kir3.1 after G431 and coexpression with wild-type Kir3.2 significantly reduced K^+ current inhibition by the two compounds and slowed the kinetics of block (Fig. 9, B, E, and F). We then examined the drug sensitivity of a chimera containing the N terminus and the transmembrane segments of Kir3.1/3.2 and the C terminus of Kir2.1. Note that the interchange of the C terminus led to more pronounced inward rectification of the chimera compared with the truncated Kir3 construct (insets in Fig. 9, B and C). Inhibition of chimera current by U73122 was significantly diminished, accompanied by a dramatic slowing of the kinetics of drug action (Fig. 9, C, E, and F). Finally, we examined how a Kir2.1 chimera containing the last part of the Kir3.1/3.2 C terminus would respond to U73122. Unlike wild-type Kir2.1, which was completely insensitive to U73122 (Fig. 3C), this chimera indeed proved sensitive to U73122 (Fig. 9, D–F).

Discussion

Our study demonstrates that U73122, a widely used PLC blocker, suppresses heterologously expressed Kir3.1/3.2 (GIRK1/2) and BK (MaxiK) channels by a mechanism that cannot be attributed to inhibition of PLC. Thus, U73122 is not an unequivocal tool to examine and dissect the role of

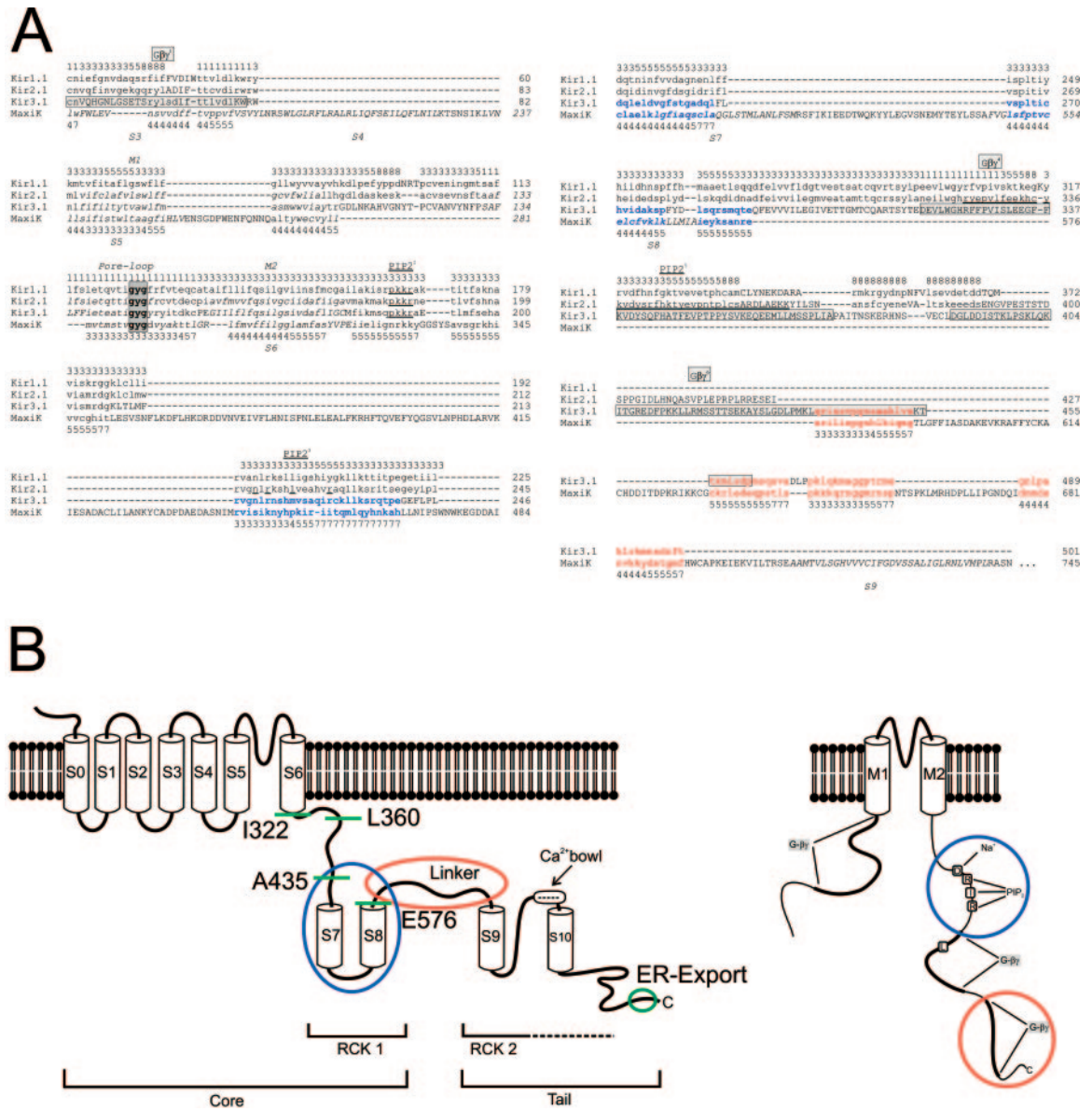

Fig. 8. Alignment of Kir1.1, Kir2.1, Kir3.1 and BK (MaxiK) reveals sequence similarities in cytoplasmic C-terminal regions of Kir3 and BK. A, secondary structure elements are noted above and below amino acid sequences (Huang et al., 1997). Numbers indicate degree of sequence homologies as calculated by MACTH-BOX software (see *Materials and Methods*). Strongest similarities in cytoplasmic C terminus were marked in blue and red. B, schematic drawings of secondary structure of BK and Kir3 channels modified after Magleby (2003) and Mark and Herlitze (2000), respectively. Blue and red circles indicate position of like-colored sequence homologies of A. Green bars indicate truncation sites for BK channel constructs. For further explanation, see text.

PLC-mediated signaling. This issue is of particular importance for voltage- and Ca^{2+}-activated BK channels, because they can be activated through the PLC-mediated breakdown of PIP_2 to IP_3, which then causes Ca^{2+} release from IP_3-sensitive intracellular Ca^{2+}-stores. Our data therefore strongly caution against the use of U73122 when exploring this pathway and add to the increasing list of unwarranted (that is PLC-independent) side effects of U73122 in the literature (see Introduction).

In principle, at least three different drug targets seem conceivable. First, the compounds might work as pore blockers. Second, they might alter channel gating by binding to a channel domain outside the pore region. Third, they might act through an adaptor protein that serves a similar function for both channels. One possibility to tackle this issue is to compare the action of U73122 with that of other inhibitors of Kir3 and/or BK channels whose mechanism of block has already been investigated. In this respect, tertiapin, a short peptide from bee venom, should be a promising candidate. Tertiapin was introduced as a specific and potent blocker of Kir3 channels at nanomolar affinity, whereas Kir2 channels remained insensitive (Jin and Lu, 1998). More recently, tertiapin was also found to inhibit BK channels (Kanjhan et al., 2005). Its mechanism of action is not fully resolved, but tertiapin is thought to occlude the channel by plugging its α helix into the external vestibule of the ion conduction pore (Jin et al., 1999). Although the pharmacological profile of tertiapin seems to match that of U73122 at first glance, some

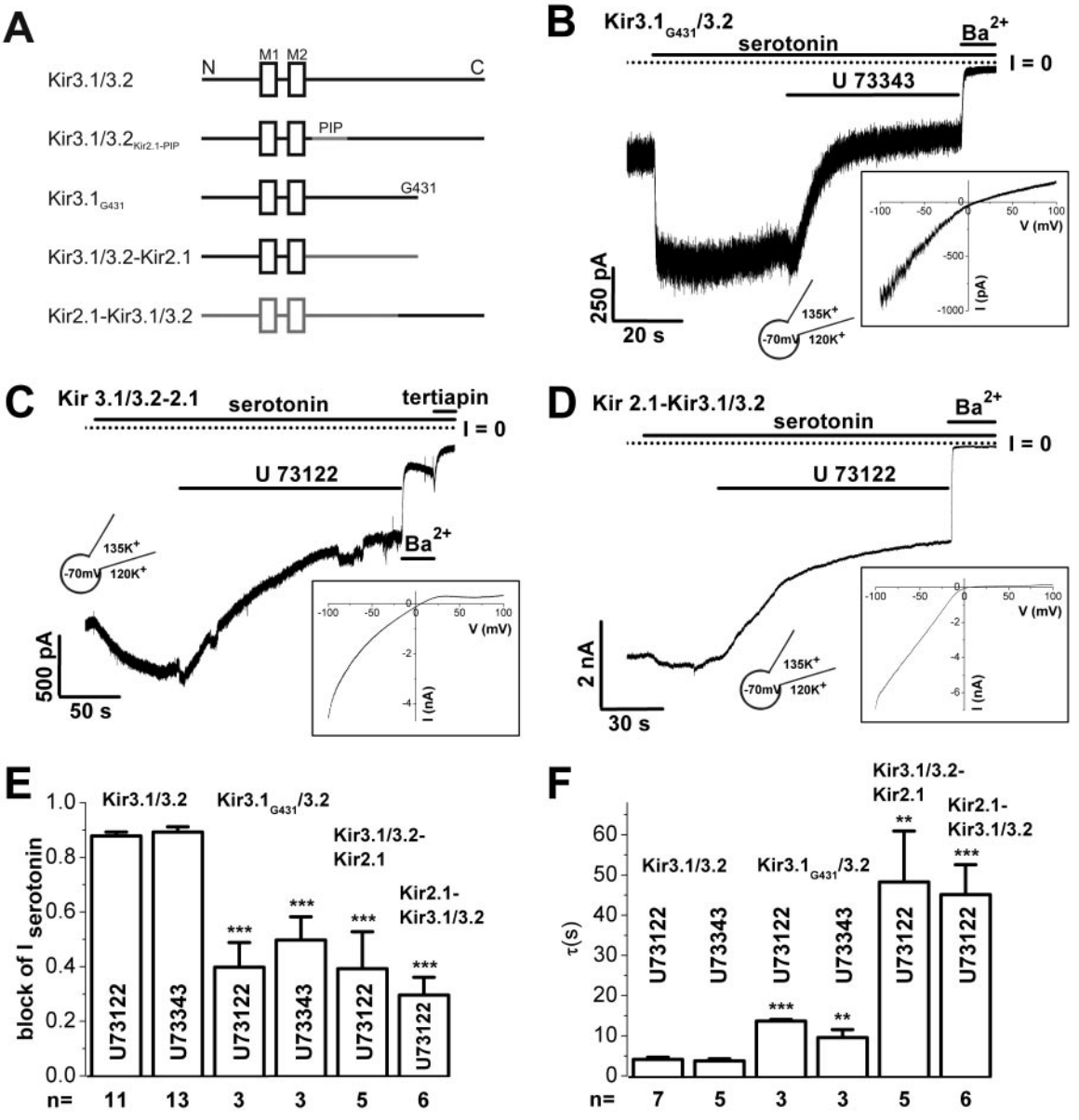

Fig. 9. Mutations in C terminus of Kir 3.1/3.2 and Kir2.1 alter sensitivity to block by U73122 and U73343. A, schematic diagram of wild-type and mutant/chimeric Kir3 and Kir2 channels. B, reduced and decelerated inhibition by U73343 (10 μM) of K^+ current generated by heteromers consisting of Kir3.1 truncated after G431 and wild-type Kir3.2. Inset depicts I-V relationship of mutant channel. C, K^+ current produced by chimera of mutant Kir3.1/3.2 channels carrying the Kir2.1 C terminus displayed reduced and slowed response to U73122 (10 μM). Inset depicts I-V relationship of mutant channel. D, in contrast to wild-type Kir2.1, K^+ current through chimera of Kir2.1 with C-terminal end region of Kir.3.1/3.2 attached displayed sensitivity to U73122 (10 μM). Inset depicts I-V relationship of mutant channel. E, summary of blocking action of U73122 and U73343 on K^+ current through wild-type and mutant channels. F, summary of time course of drug action in wild-type and mutant channels. ** $p < 0.01$, *** $p < 0.001$

clear differences have to be noted. First, unlike U73122, tertiapin is also an equally potent blocker of Kir1 channels (Jin and Lu, 1998). Second, in contrast to the inhibitory effect of U73122, block of BK channels by tertiapin is slow and use-dependent requiring strong and prolonged depolarization to develop (Kanjhan et al., 2005). Thus, tertiapin (300 nM) did not produce any suppression of BK channels when we used the same recording conditions that reliably revealed the blocking action of U73122 (physiological K^+ gradient, V_h, 0 mV; data not shown). In view of these discrepancies, the effect of U73122 on Kir3 and BK channels would be difficult to explain in terms of a direct block of the channel pore by a mechanism similar to that of tertiapin.

Cho et al. (2001) proposed that U73122 might target the PIP_2 binding site of Kir3 channels, thereby destabilizing their open state. The results of our present study do not agree with this notion, because mutations of Kir3 and Kir2 channels that strengthened and lowered PIP_2 binding, respectively, failed to alter the inhibitory effect of U73122 and U73343.

If U73122 neither plugs the pore nor interferes with PIP_2 binding, it might possibly interact with a cytoplasmic domain structure of the channel proteins. Kir3.1 and, more so, BK channels show multiple and extensive regulatory domains between their last transmembrane domains (M2 and S6, respectively) and their C-terminal ends that can be accessed by various effectors to regulate channel gating (Meera et al., 1997; Lu et al., 2006; Salkoff et al., 2006; Logothetis et al., 2007). Because all our BK constructs failed to yield viable channels, consistent with Schmalhofer et al. (2005), we designed mutant Kir3/Kir 2 channels to corroborate the hypothesis that the compounds target specific regions of the C terminus to inhibit Kir3 channel activity, as suggested by the sequence homologies between BK and Kir3 (Fig. 8). We predicted that removal of these regions from Kir3.1 or substitution with C-terminal elements of Kir2.1 should attenuate block by U73122. Vice versa, a Kir2.1 chimera containing the C terminus of Kir3.1/3.2 should be rendered sensitive to the compounds. Analysis of the respective constructs demonstrated that these predictions were indeed all confirmed (Fig. 9). These data strongly suggest that structural elements of the C terminus are prominently involved in the direct suppression of channel activity by U73122 and U73343.

One might wonder whether the unique pharmacological profile of U73343 as a selective and potent blocker of BK and Kir3 channels (without inhibiting PLC or acting as an alkylating agent), should not be exploited to devise novel compounds. In fact, suppression of both Kir3 and BK channels has already been suggested for the treatment of inflammatory and persistent pain (Kanjhan et al., 2005), and further therapeutic scenarios are conceivable. For example, the coexistence of generalized epilepsy and paroxysmal dyskinesia (GEPD) in the same individual has been attributed to a gain-of-function mutation of KCNMA1, which encodes the α-subunit of the BK channel (Du et al., 2005). Therefore, BK channel blocking agents were suggested as a potential therapy for GEPD (Du et al., 2005). How would a concomitant inhibition of Kir3 channels fit into this picture? It is worth noting that patients with GEPD display an absence-like epileptic phenotype. Absence seizures are well known to be exacerbated by $GABA_B$ receptor agonists (Marescaux et al., 1992) that in turn activate postsynaptic Kir3 channels (Sodickson and Bean, 1996; Sickmann and Alzheimer, 2002). Although counterintuitive prima facie, the simultaneous overactivity of BK and Kir3 channels might *increase* brain excitability. Potential mechanisms include faster repriming of Na^+ channels and unleashing of ion conductances such as H-current and low threshold Ca^{2+} current that initiate and augment rhythmic burst discharges, a hallmark of absence epilepsy. The concurrent pharmacological inhibition of BK and Kir3 would therefore be expected to effectively dampen this type of epileptic activity. In view of the broad spectrum of disease states that have been associated with dysfunctions of BK and Kir3 channels, novel drugs designed to selectively target these two channels might offer a promising therapeutic approach.

Acknowledgments

We thank Kerstin Kronenbitter and Didier Gremelle for technical assistance and Werner Ulbricht and Ulf-Peter Hansen for helpful discussions.

References

Cho H, Youm JB, Ryu SY, Earm YE, and Ho WK (2001) Inhibition of acetylcholine-activated K^+ currents by U73122 is mediated by the inhibition of PIP_2-channel interaction. *Br J Pharmacol* **134:**1066–1072.
Depiereux E, Baudoux G, Briffeuil P, Reginster I, De Bolle X, Vinals C, and Feytmans E (1997) Match-Box_server: a multiple sequence alignment tool placing emphasis on reliability. *Comput Appl Biosci* **13:**249–256.
Du W, Bautista JF, Yang H, Diez-Sampedro A, You SA, Wang L, Kotagal P, Lüders HO, Shi J, Cui J, et al. (2005) Calcium-sensitive potassium channelopathy in human epilepsy and paroxysmal movement disorder. *Nat Genet* **37:**733–738.
Du X, Zhang H, Lopes C, Mirshahi T, Rohacs T, and Logothetis DE (2004) Characteristic interactions with phosphatidylinositol 4,5-bisphosphate determine regulation of kir channels by diverse modulators. *J Biol Chem* **279:**37271–37281.
Filippov AK, Fernández-Fernández JM, Marsh SJ, Simon J, Barnard EA, and Brown DA (2004) Activation and inhibition of neuronal G protein-gated inwardly rectifying K^+ channels by P2Y nucleotide receptors. *Mol Pharmacol* **66:**468–477.
Horowitz LF, Hirdes W, Suh BC, Hilgemann DW, Mackie K, and Hille B (2005) Phospholipase C in living cells: activation, inhibition, Ca^{2+} requirement, and regulation of M current. *J Gen Physiol* **126:**243–262.
Huang CL, Jan YN, and Jan LY (1997) Binding of the G protein βgamma subunit to multiple regions of G protein-gated inward-rectifying K^+ channels. *FEBS Lett* **405:**291–298.
Huang CL, Slesinger PA, Casey PJ, Jan YN, and Jan LY (1995) Evidence that direct binding of G beta gamma to the GIRK1 G protein-gated inwardly rectifying K^+ channel is important for channel activation. *Neuron* **15:**1133–1143.
Huth T, Schmidtmayer J, Alzheimer C, and Hansen UP (2008) Four-mode gating model of fast inactivation of sodium channel Nav1.2a. *Pflugers Arch*, in press.
Jin W, Klem AM, Lewis JH, and Lu Z (1999) Mechanisms of inward-rectifier K^+ channel inhibition by tertiapin-Q. *Biochemistry* **38:**14294–14301.
Jin W, Lo TM, Loh HH, and Thayer SA (1994) U73122 inhibits phospholipase C-dependent calcium mobilization in neuronal cells. *Brain Res* **642:**237–243.
Jin W and Lu Z (1998) A novel high-affinity inhibitor for inward-rectifier K^+ channels. *Biochemistry* **37:**13291–13299.
Kanjhan R, Coulson EJ, Adams DJ, and Bellingham MC (2005) Tertiapin-Q blocks recombinant and native large conductance K^+ channels in a use-dependent manner. *J Pharmacol Exp Ther* **314:**1353–1361.
Kwon SH and Guggino WB (2004) Multiple sequences in the C terminus of MaxiK channels are involved in expression, movement to the cell surface, and apical localization. *Proc Natl Acad Sci U S A* **101:**15237–15242.
Lei Q, Talley EM, and Bayliss DA (2001) Receptor-mediated inhibition of G protein-coupled inwardly rectifying potassium channels involves $G\alpha_q$ family subunits, phospholipase C, and a readily diffusible messenger. *J Biol Chem* **276:**16720–16730.
Logothetis DE, Jin T, Lupyan D, and Rosenhouse-Dantsker A (2007) Phosphoinositide-mediated gating of inwardly rectifying K^+ channels. *Pflugers Arch* **455:**83–95.
Lu R, Alioua A, Kumar Y, Eghbali M, Stefani E, and Toro L (2006) MaxiK channel partners: physiological impact. *J Physiol* **570:**65–72.
Magleby KL (2003) Gating mechanism of BK (Slo1) channels: so near, yet so far. *J Gen Physiol* **121:**81–96.
Marescaux C, Vergnes M, and Bernasconi R (1992) GABAB receptor antagonists: potential new anti-absence drugs. *J Neural Transm Suppl* **35:**179–188.
Mark MD and Herlitze S (2000) G-protein mediated gating of inward-rectifier K^+ channels. *Eur J Biochem* **267:**5830–5836.
Meera P, Wallner M, Song M, and Toro L (1997) Large conductance voltage- and calcium-dependent K^+ channel, a distinct member of voltage-dependent ion channels with seven N-terminal transmembrane segments (S0–S6), an extracellular N terminus, and an intracellular (S9–S10) C terminus. *Proc Natl Acad Sci U S A* **94:**14066–14071.
Meyer T, Wellner-Kienitz MC, Biewald A, Bender K, Eickel A, and Pott L (2001) Depletion of phosphatidylinositol 4,5-bisphosphate by activation of phospholipase

C-coupled receptors causes slow inhibition but not desensitization of G protein-gated inward rectifier K^+ current in atrial myocytes. *J Biol Chem* **276:**5650–5658.
Mogami H, Lloyd Mills C, and Gallacher DV (1997) Phospholipase C inhibitor, U73122, releases intracellular Ca^{2+}, potentiates Ins(1,4,5)P3-mediated Ca^{2+} release and directly activates ion channels in mouse pancreatic acinar cells. *Biochem J* **324:**645–651.
Piskorowski R and Aldrich RW (2002) Calcium activation of BK(Ca) potassium channels lacking the calcium bowl and RCK domains. *Nature* **420:**499–502.
Salkoff L, Butler A, Ferreira G, Santi C, and Wei A (2006) High-conductance potassium channels of the SLO family. *Nat Rev Neurosci* **7:**921–931.
Schmalhofer WA, Sanchez M, Dai G, Dewan A, Secades L, Hanner M, Knaus HG, McManus OB, Kohler M, Kaczorowski GJ, et al. (2005) Role of the C-terminus of the high-conductance calcium-activated potassium channel in channel structure and function. *Biochemistry* **44:**10135–10144.
Schroeder I and Hansen UP (2007) Saturation and microsecond gating of current indicate depletion-induced instability of the MaxiK selectivity filter. *J Gen Physiol* **130:**83–97.
Sickmann T and Alzheimer C (2002) Agonist-specific maturation of GIRK current responses in acutely isolated pyramidal neurons of rat neocortex. *Brain Res* **929:**166–174.
Sickmann T and Alzheimer C (2003) Short-term desensitization of G-protein-activated, inwardly rectifying K^+ (GIRK) currents in pyramidal neurons of rat neocortex. *J Neurophysiol* **90:**2494–2503.
Sickmann T, Klose A, Huth T, and Alzheimer C (2008) Unexpected suppression of neuronal G protein-activated, inwardly rectifying K^+ current by common phospholipase C inhibitor. *Neurosci Lett* **436:**102–106.
Slesinger PA, Reuveny E, Jan YN, and Jan LY (1995) Identification of structural elements involved in G protein gating of the GIRK1 potassium channel. *Neuron* **15:**1145–1156.
Sodickson DL and Bean BP (1996) $GABA_B$ receptor-activated inwardly rectifying potassium current in dissociated hippocampal CA3 neurons. *J Neurosci* **16:**6374–6385.
Sodickson DL and Bean BP (1998) Neurotransmitter activation of inwardly rectifying potassium current in dissociated hippocampal CA3 neurons: Interactions among multiple receptors. *J Neurosci* **18:**8153–8162.
Vickers JD (1993) U73122 affects the equilibria between the phosphoinositides as well as phospholipase C activity in unstimulated and thrombin-stimulated human and rabbit platelets. *J Pharmacol Exp Ther* **266:**1156–1163.
Zhang H, He C, Yan X, Mirshahi T, and Logothetis DE (1999) Activation of inwardly rectifying K^+ channels by distinct PtdIns(4,5)P2 interactions. *Nat Cell Biol* **1:**183–188.
Zhou W, Arrabit C, Choe S, and Slesinger PA (2001) Mechanism underlying bupivacaine inhibition of G protein-gated inwardly rectifying K^+ channels. *Proc Natl Acad Sci U S A* **98:**6482–6487.

Address correspondence to: Dr. Christian Alzheimer, Department of Physiology, University of Kiel, Olshausenstr. 40, 24098 Kiel, Germany. E-mail: c.alzheimer@physiologie.uni-kiel.de